Front. Optoelectron. 2016, 9(3): 489–496
DOI 10.1007/s12200-016-0560-0

RESEARCH ARTICLE

Route-asymmetrical light transmission of a fiber-chip-fiber optomechanical system

Li LIU[1], Yunhong DING[2], Xinlun CAI[3,4], Jianji DONG (✉)[1], Xinliang ZHANG[1]

1 Wuhan National Laboratory for Optoelectronics (WNLO), Huazhong University of Science and Technology, Wuhan 430074, China
2 Department of Photonics Engineering, Technical University of Denmark, 2800 Kgs. Lyngby, Denmark
3 State Key Laboratory of Optoelectronic Materials and Technologies, School of Physics and Engineering, Sun Yatsen University, Guangzhou 510275, China
4 Centre for Quantum Photonics, H. H. Wills Physics Laboratory, Department of Electrical and Electronic Engineering, University of Bristol, Bristol BS8 1UB, UK

Abstract In this paper, we proposed and experimentally demonstrated a route-asymmetrical light transmission scheme based on the thermal radiative effect, which means that forward and backward propagations of an optical device have different transmittances provided they are not present simultaneously. Employing a fiber-chip-fiber optomechanical system, our scheme has successfully achieved a broad operation bandwidth of at least 24 nm and an ultra-high route-asymmetrical transmission ratio (RATR) up to 63 dB. The route-asymmetrical device has been demonstrated effectively with not only the continuous-wave (CW) light but also 10 Gbit/s on-off-keying (OOK) digital signals. Above mentioned unique features can be mostly attributed to the significant characteristics of the thermal radiative effect, which could cause a fiber displacement up to tens of microns. The powerful and significant thermal radiative effect opens up a new opportunity and method for route-asymmetrical light transmission. Moreover, this research may have important applications in all-optical systems, such as the optical limiters and ultra-low loss switches.

Keywords route-asymmetrical light transmission, thermal radiative effect, optomechanical system, route-asymmetrical transmission ratio (RATR)

1 Introduction

The function to control the transmission directions of optical signals is a fundamental research and in great demand in optical communication and processing systems [1–10]. One important and effective implemention is the route-asymmetrical light transmission which means that forward and backward propagations of an optical device have different transmittances provided they are not present simultaneously [11]. Nowadays, this function has already been widely used in optical information processing systems, such as optical diodes [12], logic gates [13,14] and switches [15–17]. To pursue more satisfying route-asymmetrical performances, a number of innovative route-asymmetrical devices based on different physical mechanisms have been conceived. However, different major unfavorable factors have not been adequately eliminated in these schemes. For example, researchers have made great efforts to achieve route-asymmetrical devices of low cost and simple operation based on the material nonlinearity of the microcavities [18–22] and thermal effect [23,24], but most of the operation bandwidths are too narrow. Devices relying on the optical force largely improve the operation bandwidth, however they also bring additional complexity to the fabrication and operation process [10]. As for schemes based on the refractive index modulation [25], spatial mode converter [26] and light tunneling mechanism in heterostructures [27], either the system complexity or unsatisfied route-asymmetrical performance, seriously limits their applications in next-generation optical communication systems [28,29]. Therefore, it is significant to find an effective mechanism to simplify the fabrication and operation process, and improve the transmission performances of route-asymmetrical system for practical applications.

Considering the packaging of photonic circuits, integrated chips have inevitably been linked with optical fibers for real deployments. Hence, in this paper, by employing a fiber-chip-fiber optomechanical system, we experimentally

Received October 2, 2015; accepted December 9, 2015

E-mail: jjdong@mail.hust.edu.cn

demonstrate a route-asymmetrical light transmission scheme based on the thermal radiative effect. By taking advantage of the significant thermal radiative effect to introduce asymmetric displacements of the forward and backward fibers, our experiment shows a broad operation bandwidth of at least 24 nm and an ultra-high route-asymmetrical transmission ratio (RATR) up to 63 dB. The route-asymmetrical device has been demonstrated effectively with not only the continuous-wave (CW) light but also 10 Gbit/s non-return-to-zero on-off-keying (NRZ-OOK) digital signals. Besides the common features of the passive characteristic, broad operation bandwidth and ultra-high RATR, the proposed scheme does not require extra assistance, such as electro-optic modulation or external optical pumping. Moreover, this scheme may have significant applications in all-optical switches and limiters.

2 Device fabrication and operation principle

Figure 1(a) provides an insight into the structure of our fiber-chip-fiber optomechanical system, which includes a pair of lensed single-mode fibers side-coupled to a silicon straight waveguide chip. The forward fiber is totally fixed by the fixtures, while the backward fiber is half fixed with the coupling end designed with a suspended length of several centimeters, behaving as a movable fiber cantilever structure. The coupling ends of the two fibers are both bare without coatings and tilted at an angle of 12° for optimal coupling. Figure 1(b) shows the scanning electron microscope (SEM) image of one grating coupler, which is fabricated on a commercial silicon-on-insulator (SOI) wafer. The top silicon thickness of the SOI wafer is 340 nm, and the buried oxide layer thickness is 2 μm. The device layout is transferred to a ZEP520A photoresist using E-beam lithography (Vistec EBPG5000 + ES). Then, the upper silicon layer is etched downward of 210 nm to form a ridge waveguide through inductively coupled plasma (ICP) etching (Oxford Instruments Plasmalab System100). The period, duty cycle, total length, 3-dB coupling bandwidth and coupling loss for a single side of the grating coupler are 630 nm, 56%, 19 μm, 30 nm (ranging from 1535 to 1565 nm) and 9 dB, respectively.

The working principle of the proposed route-asymmetrical light transmission can be described as follows. When a strong CW light is injected into the backward fiber, the scattered light power due to the imperfect coupling between the fiber and the grating coupler will produce a thermal radiative effect which could make the backward fiber move away. Thus the light transmission would be blocked. In contrast, for the forward input, there is no displacement of the two fibers (or a small displacement, but this is within the tolerance of the grating couplers). The reason for this is that the forward fiber is fixed stably and the light, experiencing a relatively high loss mainly induced by the grating coupler, is not strong enough to generate a powerful thermal radiative effect at the backward port. Thus the backward fiber also keeps stable. In this case, the fiber-chip-fiber system can be regarded as a lossy linear system and the CW light could transmit to the backward fiber. Therefore, the fiber-chip-fiber optomechanical system provides a successful design for route-asymmetrical light transmission.

3 Experimental results

3.1 Route-asymmetrical performance with the backward suspended length of 1.8 cm

At first, the suspended length of the backward fiber was set

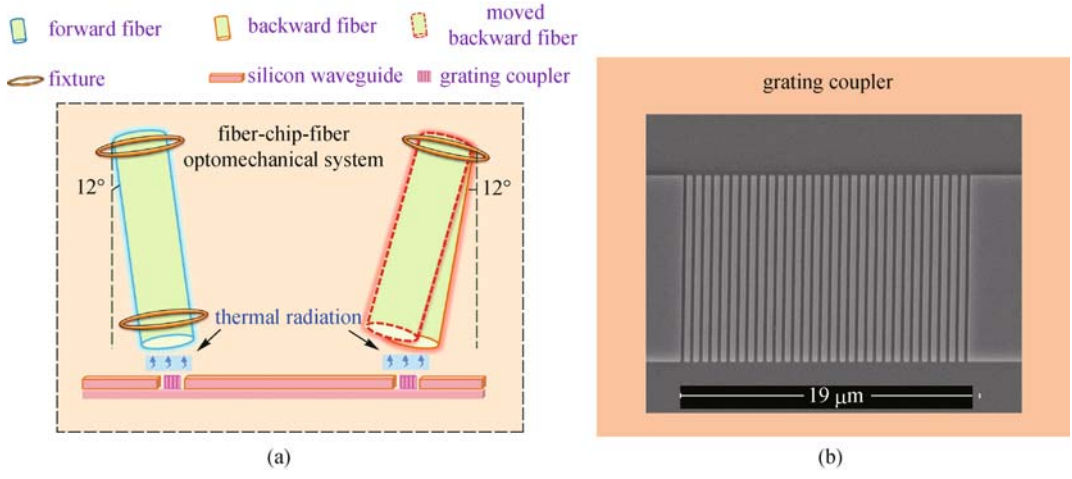

Fig. 1 Structure of the route-asymmetrical system. (a) Schematic illustration of the fiber-chip-fiber optomechanical system consisting of a silicon straight waveguide and a pair of single-mode fibers; (b) SEM image of the silicon grating coupler

at 1.8 cm. To investigate the route-asymmetrical behavior of the optomechanical device, the wavelength and power of the input CW light were adjusted to 1550 nm and 20 dBm, respectively. When the light was separately injected from the forward and backward fibers, the output power was measured as 1.5 and –43.5 dBm, respectively. Hence, the RATR, defined as the difference (in dB unit) between the forward transmission power (T_F) and the backward transmission power (T_B), was about 45 dB. To explore the operation bandwidth of this device, we scanned the input optical wavelength covering the whole C band and repeated the above measurements. As shown in Fig. 2(a), most of the RATRs ($T_F - T_B$ in dB unit) were larger than 40 dB when the wavelength ranged from 1536 to 1560 nm, showing a route-asymmetrical working bandwidth of at least 24 nm.

To further investigate the impact of input power on the performance of this system, we fixed the optical wavelength at 1550 nm and varied the input power from 6 to 20 dBm. For the forward transmission, we found that the output power increased linearly with the input power, shown as the blue line in Fig. 2(b). For the backward transmission, the output power also increased linearly with the input power when the input power was lower than 12 dBm. However, over this threshold, the output power drastically reduced all the way with increasing the input power, shown as the red line in Fig. 2(b). Hence, a large range of input powers to achieve high RATRs was successfully obtained, with the largest RATR of 45 dB.

3.2 Improved route-asymmetrical performance with increasing the backward suspended length to 2.0 cm

As the route-asymmetrical performance was dependent on the displacement of the backward fiber, we increased the suspended length to 2.0 cm in order to enhance the system sensibility with a lower power operation. Here the light wavelength was fixed at 1550 nm. Figure 3(a) showed the measured backward and forward transmissions under different input powers. The maximum RATR increased to 63 dB, which was larger than the case of Fig. 2(b).

We also investigated the relationships between the fiber displacements and the input powers for the backward injection, as shown in Fig. 3(b). For example, when the backward incident power was 20 dBm, the movable fiber completely deviated from the grating coupler with a displacement up to 38μm, which was twice the length of the grating coupler. Figures 3(c)–3(e) presented the corresponding positions of the movable fiber at different input powers, which were recorded by a charge coupled device (CCD) camera. When the input light power was 9 dBm, the generated thermal radiative effect was not strong enough, and hence the fiber was still accurately aligned with the grating coupler, as shown in Fig. 3(c). As the input power was increased to 17 dBm, Fig. 3(d) showed that the backward fiber obviously moved a long distance, which led to high light loss. Once the input power was enhanced to 20 dBm, Fig. 3(e) showed that the backward fiber completely deviated from the grating coupler, and the light transmission was cut off.

Considering the displacement magnitude and material characteristics of the optical fiber, the movement of backward fiber could be mostly attributed to the thermal expansion of the fiber [30–32]. When a strong CW light is injected into the backward fiber, the high power will be partly scattered by the grating coupler because of the imperfect coupling between the fiber and the grating coupler, which could significantly increase the temperature of the grating coupler. Then the infrared power emitted by the hot grating is absorbed by the cladding layer of the backward fiber which makes the lower side of the fiber is hotter. As a result, the backward fiber would be deformed due to the thermal nonequilibrium, and thereafter produce a displacement. In other words, the movement of the

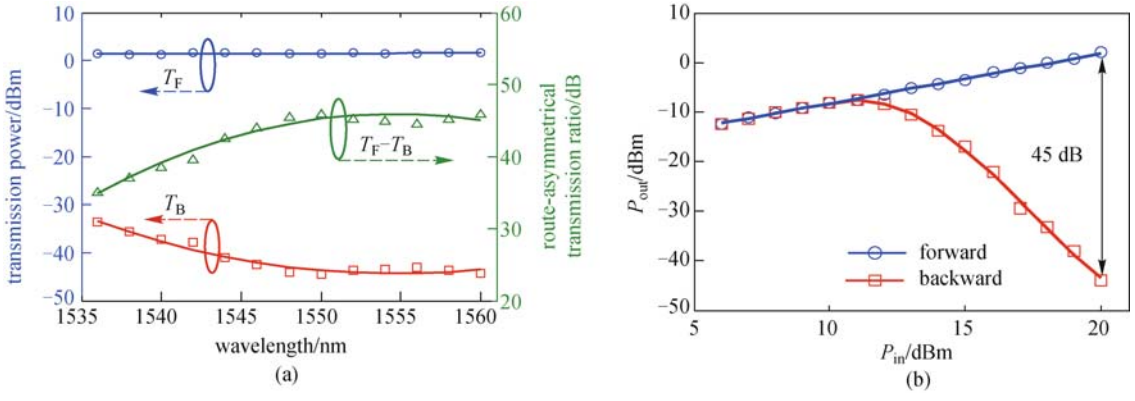

Fig. 2 Route-asymmetrical performance with a suspended length of 1.8 cm for the backward fiber. (a) Broad bandwidth with an input light power of 20 dBm. The forward transmission power (T_F) and the backward transmission power (T_B) were shown as the blue and red curves, respectively. The green line, which was the difference between them, was defined as the RATR (T_F–T_B in dB unit); (b) route-asymmetrical condition with an input light wavelength of 1550 nm. The forward and backward output powers, as functions of the input powers, were fitted as the blue and red curves, respectively

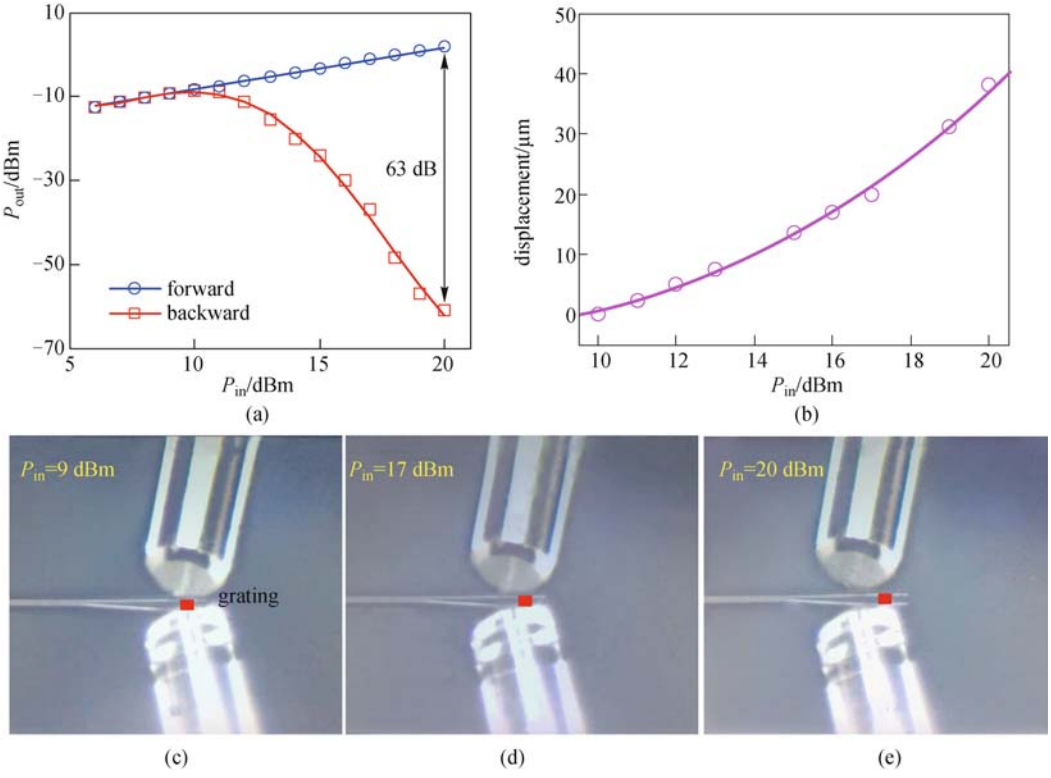

Fig. 3 Route-asymmetrical performance when the suspended length of the backward fiber was increased to 2.0 cm. (a) Higher measured RATRs; (b) measured displacements of the backward fiber under different input powers; (c)–(e) position images of the backward fiber under the input power of (c) 9 dBm, (d) 17 dBm and (e) 20 dBm. With increasing the input power, the backward fiber gradually moved away from the grating coupler, which was marked as the red region. In (c), (d) and (e), one fiber was the actual object, while the other was its virtual image

backward fiber might be caused by the thermal radiative effect which was the leading factor in a conversion process between different energies (from the original scattered light energy to the final mechanical energy of the backward fiber).

In the future, the operation power of the proposed device could be reduced by designing an improved system which could more efficiently realize energy conversion from the scattered light power to the mechanical energy. At first, we could increase the suspended length of the backward fiber to enhance the system sensitivity. In this case, devices with less operation power could achieve the same route-asymmetrical performances. Second, we could use other materials or structures which could be more sensitive to the thermal radiative effect instead of the fibers. For example, we could fabricate the on-chip counterpart of the proposed device so as to reduce the weight of the movable part. Once we have designed the movable backward part with a compact and light material, i.e., SOI cantilever waveguide instead of the backward fiber, the required optical power will be greatly reduced. Furthermore, as the proposed device is independent of the laser wavelength, the route-asymmetrical bandwidth can be greatly increased by designing a grating coupler with a larger bandwidth [33,34].

3.3 Route-asymmetrical performance of 10 Gbit/s modulation signal

To verify whether this proposed device can work well with digital modulation signals, we carried out an experiment, as shown in Fig. 4. A CW light of 10 dBm power, emitted from a tunable laser source (TLS), was modulated by cascaded Mach-Zehnder modulators (MZMs). Meanwhile, a bit pattern generator (BPG) appropriately drove the MZMs to produce 10 Gbit/s NRZ-OOK signals. Then, a high-power erbium-doped fiber amplifier (HP-EDFA) was used to pump the modulated NRZ signals, and then a variable optical attenuator (VOA) was used to adjust the injection power. The polarization controller 2 (PC2) was required, since the silicon waveguide operated only in the transverse electrical (TE) mode. A communication signal analyzer (CSA) was used to record the temporal waveforms.

The suspended length of the backward fiber and the optical wavelength were fixed at 2.0 cm and 1550 nm, respectively. With input powers of 10, 12, 17 and 20 dBm respectively, Figs. 5(a1)–(d1) showed that the corresponding waveform amplitudes in the time domain of the forward transmission increased accordingly. However, the waveforms of the backward transmission gradually

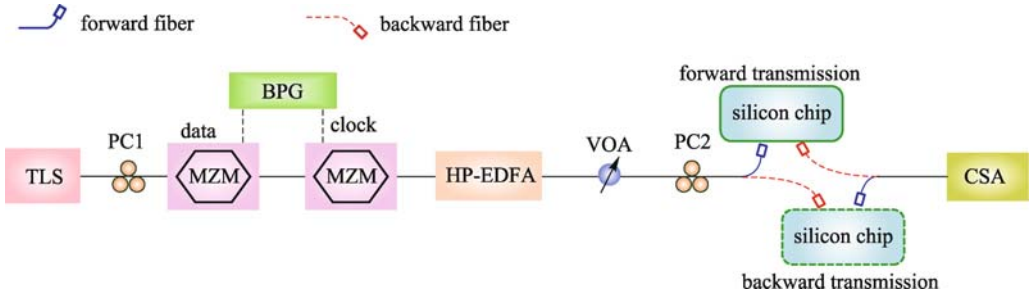

Fig. 4 Experimental setup with 10 Gbit/s NRZ signals. The components of the apparatus were labeled as follows: TLS, tunable laser source; PC, polarization controller; MZM, Mach-Zehnder modulator; BPG, bit pattern generator; HP-EDFA, high-power erbium-doped fiber amplifier; VOA, variable optical attenuator; CSA, communication signal analyzer

disappeared, as shown in Figs. 5(a2) – (d2).

Figure 6 presented the measured output average power of the NRZ signals as a function of the input average power in both the forward and backward transmissions. When the input power was increased to 20 dBm, the RATR reached its maximum value of 56 dB. These results demonstrated that this device was also effective for high-speed digital modulation signals with high route-asymmetrical performance.

The essential reason for this could be traced, as the optomechanical effect was a low-frequency mechanical oscillation which could not respond to the high-speed optical signals. Obviously, the forward light transmission was always unobstructed. However, when a strong enough light was injected at high speed into the backward fiber, there was a significant average power of high-frequency acting at the backward grating coupler, which was equivalent to continuous excitation. In this case, the backward fiber deviated away from the grating coupler and cut off the light. Hence, the proposed device can also work well with high-speed digital signals.

3.4 Reflectivity

As the reflectivity was an important performance index for practical devices[1)], Fig. 7 showed the measured reflectivity of the forward port (R_F) and backward port (R_B) as a function of the input powers when the input wavelength was 1550 and 1545 nm respectively. The forward reflectivity (red lines in Fig. 7) was approximately constant and lower than 0.5% when the input power varied from 8 to 22 dBm. However, the backward reflectivity (blue lines in Fig. 7) increased with the input power and finally tended to be steady around 1.3%. The reason lay in that with the

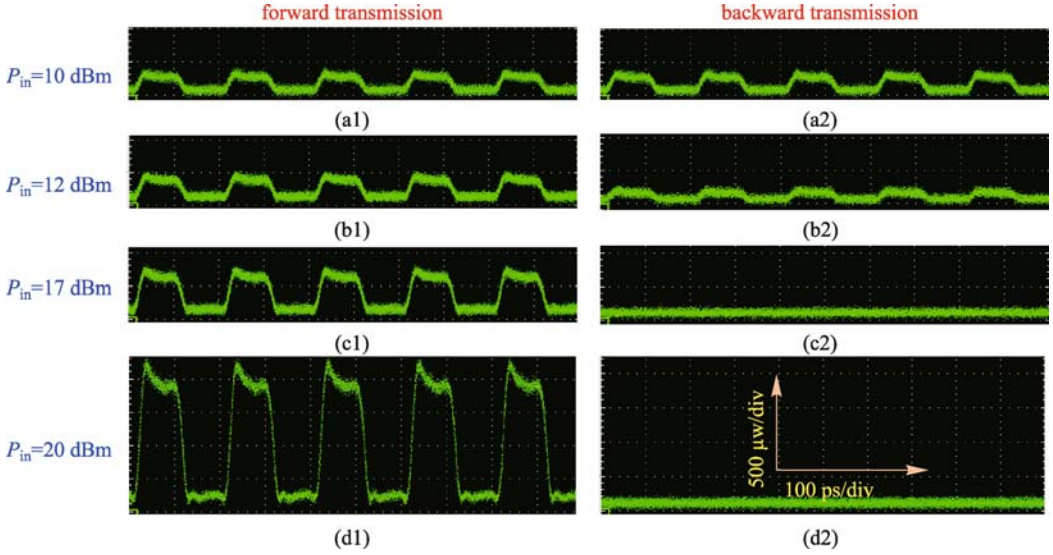

Fig. 5 Time domain waveforms of the NRZ signals under various input powers. In forward transmission, the output NRZ signals with input powers of (a1) 10 dBm, (b1) 12 dBm, (c1) 17 dBm and (d1) 20 dBm. In backward transmission, the output signals with input powers of (a2) 10 dBm, (b2) 12 dBm, (c2) 17 dBm and (d2) 20 dBm in backward propagation. The scales of time coordinate and the power amplitude of the output signal were 100 ps/div and 500 μw/div, respectively

1) https://en.wikipedia.org/wiki/Reflectance#Reflectivity

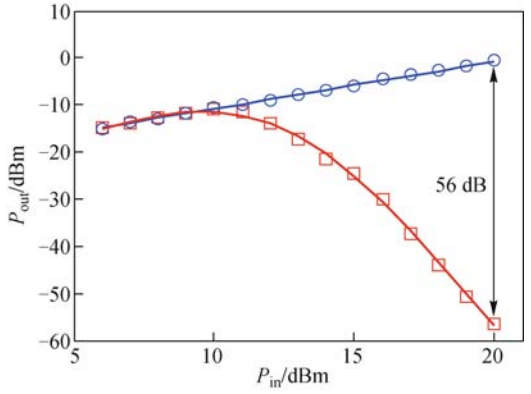

Fig. 6 RATRs of the NRZ signal. The RATRs of the forward and backward transmissions were plotted as the blue and red curves, respectively

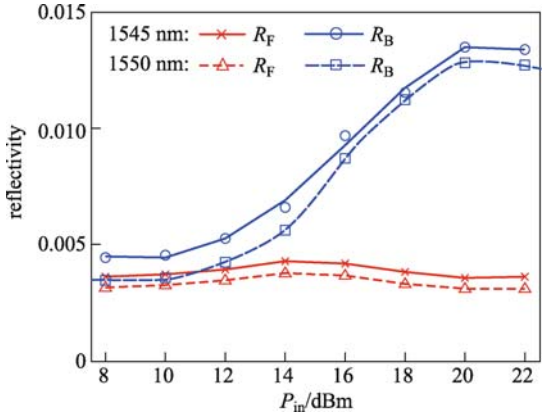

Fig. 7 Reflectivity of the forward port (R_F) and backward port (R_B) under different input powers and wavelengths

movement of the backward fiber, less light coupled into the gratings which resulted in more optical power reflection. After the fiber moved to the farthest position and turned to be steady, the backward reflectivity stopped increasing and remained unchanged at a level of lower than 1.5%. Therefore, the reflectivity of this route-asymmetrical device was acceptable for practical applications.

According to above measured results, it is clear to see that the thermal radiative effect has a high value of practical application. It should be noted that our scheme can be incorporated into other integrated photonic circuits to realize advanced functional modules, by replacing the silicon straight waveguide with other functional waveguides to build a unidirectional functional module.

Our scheme is a semi-integration structure, but the powerful thermal radiative force is promising to be used in complete on-chip devices in the future. For example, the switching function of the backward fiber could be instead of a movable cantilever waveguide in SOI platform whose buried oxide layer is etched. In this design, by controlling the on-off state of the movable waveguide in different transmission directions, on-chip route-asymmetrical light transmission could be realized based on the thermal radiative effect. In addition, as the whole device is fabricated on the SOI wafer, it could be packaged in a closed environment to avoid some unfavorable factors (such as the vibrational fluctuations) as possible.

3.5 Practical applications for optical limiters or switches

Besides the application of route-asymmetrical transmission, our scheme could be used as a power limiter in linear optics that converts specific kinds of inputs to specific kinds of outputs [35,36]. The suspended fiber and the grating coupler could be engineered to limit the input power below a certain threshold in order to avoid the nonlinear optical effects in linear optical chips. Moreover, this scheme can still be used as an optical switch with ultra-low loss by employing a control light of strong power and grating coupler of ultra-low loss, such as the grating of 0.58-dB loss [33]. In this case, the wavelength of the control light should be out of the working bandwidth of the grating coupler in order to introduce strong thermal radiative effect, while the signal light is within the bandwidth of the grating coupler and could efficiently couple into the device. Once the transmission link is required to cut off the signals, we only need to increase the power of the control light. In this way, an optical mechanical switch of ultra-low loss could be built.

4 Conclusions

We have experimentally demonstrated a route-asymmetrical light transmission in a fiber-chip-fiber optomechanical system based on the thermal radiative effect. The scheme is effective at achieving a broad operation bandwidth of at least 24 nm and an ultra-high RATR up to 63 dB. This route-asymmetrical device has been demonstrated effectively with not only the CW light but also 10 Gbit/s OOK digital signals. Moreover, this research may have significant applications in all-optical systems, such as the optical limiters and ultra-low loss switches. Our findings of fiber optomechanical effect may motivate the applications of on-chip optomechanical system.

Acknowledgements This work was partially supported by the National Basic Research Program of China (No. 2011CB301704), the Program for New Century Excellent Talents in Ministry of Education of China (No. NCET-11-0168), a Foundation for the Author of National Excellent Doctoral Dissertation of China (No. 201139), the National Natural Science Foundation of China (Grant Nos. 11174096 and 61475052), and the Opened Fund of the State Key Laboratory on Advanced Optical Communication System and Network (No. 2015GZKF03004).

References

1. Bi L, Hu J, Jiang P, Kim D H, Dionne G F, Kimerling L C, Ross C A. On-chip optical isolation in monolithically integrated non-reciprocal optical resonators. Nature Photonics, 2011, 5(12): 758–762
2. Shoji Y, Mizumoto T, Yokoi H, Hsieh I, Osgood R M. Magneto-optical isolator with silicon waveguides fabricated by direct bonding. Applied Physics Letters, 2008, 92(7): 071117-1–071117-3
3. Espinola R L, Izuhara T, Tsai M, Osgood R M , Dötsch H. Magneto-optical nonreciprocal phase shift in garnet/silicon-on-insulator waveguides. Optics Letters, 2004, 29(9): 941–943
4. Yokoi H, Mizumoto T, Shinjo N, Futakuchi N, Nakano Y. Demonstration of an optical isolator with a semiconductor guiding layer that was obtained by use of a nonreciprocal phase shift. Applied Optics, 2000, 39(33): 6158–6164
5. Manipatruni S, Robinson J T, Lipson M. Optical nonreciprocity in optomechanical structures. Physical Review Letters, 2009, 102(21): 213903-1–213903-4
6. Shi Y, Yu Z, Fan S. Limitations of nonlinear optical isolators due to dynamic reciprocity. Nature Photonics, 2015, 9(6): 388–392
7. Kang M S, Butsch A, Russell P S J. Reconfigurable light-driven opto-acoustic isolators in photonic crystal fibre. Nature Photonics, 2011, 5(9): 549–553
8. Lira H, Yu Z, Fan S, Lipson M. Electrically driven nonreciprocity induced by interband photonic transition on a silicon chip. Physical Review Letters, 2012, 109(3): 033901-1–033901-5
9. Yu Z, Fan S. Complete optical isolation created by indirect interband photonic transitions. Nature Photonics, 2009, 3(2): 91–94
10. Aman H, Hussain B, Aman A. Laser diode corner pumped Nd: KGW slab laser. Frontiers of Optoelectronics, 2014, 7(1): 107–109
11. Min S, Liao S, Zou C, Zhang X, Dong J. Route-asymmetrical optical transmission and logic gate based on optical gradient force. Optics Express, 2014, 22(21): 25947–25952
12. Gallo K, Assanto G, Parameswaran K R, Fejer M M. All-optical diode in a periodically poled lithium niobate waveguide. Applied Physics Letters, 2001, 79(3): 314–316
13. Xu Q, Lipson M. All-optical logic based on silicon micro-ring resonators. Optics Express, 2007, 15(3): 924–929
14. Xu Q, Soref R. Reconfigurable optical directed-logic circuits using microresonator-based optical switches. Optics Express, 2011, 19(6): 5244–5259
15. Chu T, Yamada H, Ishida S, Arakawa Y. Compact $1 \times N$ thermo-optic switches based on silicon photonic wire waveguides. Optics Express, 2005, 13(25): 10109–10114
16. Notomi M, Shinya A, Mitsugi S, Kira G, Kuramochi E, Tanabe T. Optical bistable switching action of Si high-Q photonic-crystal nanocavities. Optics Express, 2005, 13(7): 2678–2687
17. Pruessner M W, Stievater T H, Ferraro M S, Rabinovich W S. Thermo-optic tuning and switching in SOI waveguide Fabry-Perot microcavities. Optics Express, 2007, 15(12): 7557–7563
18. Fan L, Wang J, Varghese L T, Shen H, Niu B, Xuan Y, Weiner A M, Qi M. An all-silicon passive optical diode. Science, 2012, 335 (6067): 447–450
19. Fan L, Varghese L T, Wang J, Xuan Y, Weiner A M, Qi M. Silicon optical diode with 40 dB nonreciprocal transmission. Optics Letters, 2013, 38(8): 1259–1261
20. Tocci M D, Bloemer M J, Scalora M, Dowling J P, Bowden C M. Thin-film nonlinear optical diode. Applied Physics Letters, 1995, 66 (18): 2324–2326
21. Zhang Y, Li D, Zeng C, Huang Z, Wang Y, Huang Q, Wu Y, Yu J, Xia J. Silicon optical diode based on cascaded photonic crystal cavities. Optics Letters, 2014, 39(6): 1370–1373
22. Soljačić M, Luo C, Joannopoulos J D, Fan S. Nonlinear photonic crystal microdevices for optical integration. Optics Letters, 2003, 28 (8): 637–639
23. Almeida V R, Lipson M. Optical bistability on a silicon chip. Optics Letters, 2004, 29(20): 2387–2389
24. Wurtz G A, Pollard R, Zayats A V. Optical bistability in nonlinear surface-plasmon polaritonic crystals. Physical Review Letters, 2006, 97(5): 057402-1–057402-4
25. Wang D, Zhou H, Guo M, Zhang J, Evers J, Zhu S. Optical diode made from a moving photonic crystal. Physical Review Letters, 2013, 110(9): 093901-1–093901-5
26. Liu V, Miller D A B, Fan S. Ultra-compact photonic crystal waveguide spatial mode converter and its connection to the optical diode effect. Optics Express, 2012, 20(27): 28388–28397
27. Xue C, Jiang H, Chen H. Highly efficient all-optical diode action based on light-tunneling heterostructures. Optics Express, 2010, 18 (7): 7479–7487
28. Xu J, Zhuang X, Guo P, Huang W, Hu W, Zhang Q, Wan Q, Zhu X, Yang Z, Tong L, Duan X, Pan A. Asymmetric light propagation in composition-graded semiconductor nanowires. Scientific Reports, 2012, 2(11): 820-1–820-7
29. Wang J. A special issue on *Information Optoelectronics*: *Devices, Technologies and Applications*. Frontiers of Optoelectronics, 2014, 7(3): 263–264
30. Wachter E A, Thundat T, Oden P I, Warmack R J, Datskos P G, Sharp S L. Remote optical detection using microcantilevers. Review of Scientific Instruments, 1996, 67(10): 3434–3439
31. Datskos P G, Lavrik N V, Rajic S. Performance of uncooled microcantilever thermal detectors. Review of Scientific Instruments, 2004, 75(4): 1134–1148
32. Lavrik N V, Sepaniak M J, Datskos P G. Cantilever transducers as a platform for chemical and biological sensors. Review of Scientific Instruments, 2004, 75(7): 2229–2253
33. Ding Y, Peucheret C, Ou H, Yvind K. Fully etched apodized grating coupler on the SOI platform with -0.58 dB coupling efficiency. Optics Letters, 2014, 39(18): 5348–5350
34. Taillaert D, Bienstman P, Baets R. Compact efficient broadband grating coupler for silicon-on-insulator waveguides. Optics Letters, 2004, 29(23): 2749–2751
35. Miller D A B. All linear optical devices are mode converters. Optics Express, 2012, 20(21): 23985–23993
36. Miller D A B. Self-aligning universal beam coupler. Optics Express, 2013, 21(5): 6360–6370

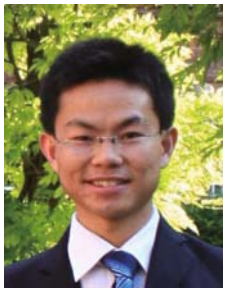

Jianji Dong is professor in Wuhan National Laboratory for Optoelectronics, Huazhong University of Science and Technology (HUST), Wuhan, China. He is working on the silicon photonics, photonic computing, and microwave photonics. He is an Editorial Board Member of *Scientific Reports*. He received the National Best Dissertations Award in 2010 and the first award of Natural Science of Hubei Province in 2013.